INFLUENCES OF DEMAGNETIZING FREQUENCY AND MAGNETIZING CONDITION ON IRON LOSSES IN SILICON-IRON TAPE-WOUND CORES

by
Kaneo MOHRI
(Received October 31, 1975)

Abstract—The loss-per-cycle versus magnetizing frequency characteristic of grain-oriented silicon-iron tape-wound cores with various demagnetizing frequency and magnetizing conditions is analysed by using a model for dynamic domain size variation which results in a minimum value for total energy. The optimum tape thickness, at which the iron loss is minimum , is also calculated using a wall-pinning model.

Notation

2a	domain-wall spacing (cm)
d	tape thickness (cm)
f	magnetizing frequency (Hz)
f_{dem}	demagnetizing frequency (Hz)
n	odd integer
y_m	maximum surface displacement of domain wall (cm)
B_m	peak flux density
B_s	saturation flux density
L_{mean}	mean length of a bowing domain wall over a cycle (cm)
M_s	saturation magnetization
W_e	eddy-current loss
W_h	hysteresis loss
W_i	iron loss
ε_m	mean energy per unit area of a bowing domain wall over a cycle (ergs / cm²)
μ	quasi-static permeability as a function of peak flux density
μ_{dv}	μ_d in the case of "voltage excitation"

Associate Professor at the Dept. of Electrical Engineering. Kyushu Institute of Technology.

$\mu_{\Delta c}$	μ_{Δ} in the case of "current excitation"
ρ	resistivity (emu)
ω	angular frequency (rad / s)
ω^*	magnetic pole desity at grain boundaries
Σ'	summation over odd integers

1. INTRODUCTION

The discrepancy between the total measured power loss and the sum of the static hysteresis loss and classical eddy-current loss has been termed the anomalous loss in grain-oriented silicon-iron and is, in present day material, responsible for large part of the total loss. The increasing importance of the anomalous loss has been due to two major causes, namely, improvements in the material, which decreased the static hysteresis loss, and a greater knowledge of the shape of the loss-per-cycle against frequency characteristic.

It has been pointed out by Williams, Shockley, and Kittel [1] (1950), that the anomalous loss could in principle be accounted for if the domain structure was considered in the loss calculation. Pry and Bean [2] (1958) calculated the relationship between the eddy current loss against various ratio of domain spacing to sheet thickness by using a model consists of equal width, planar 180° domain walls oscillating at equilibrium positions. Lee [3] (1960) also analysed the eddy current loss as a function of arbitrary dynamic domain size, exciting frequency, and the amplitude of small sinusoidal field by using a model consists of constant permeability, equal width 180° walls which are bowed by high-frequency field. In later experiments [4,5,6], the decreasing of average dynamic domain size with increasing magnetization frequency and / or peak flux density in a 3% Si-Fe single crystal was observed by using Kerr magneto-optic effect, although the reason for this was not apparent.

The mechanism of dynamic domain size variation is analysed by Haller and Kramer [7] (1970) and Sharp and Horner [8] (1973) for 3% Si-Fe single crystals. Haller and Kramer accurately predicted their experimental result, such that the average domain width is found to vary with frequency as $(f)^{-1/2}$ and with peak flux density as $(B_m)^{-1}$ above a threshold frequency and above a threshold flux density respectively in a rectangular single-crystal specimen of an 3% Si-Fe alloy, by an application of the principle of minimum entropy production. However, the domain spacing, constant in region below a threshold frequency in experiment, goes to infinity as f approaches zero. Sharp and Horner explained the low frequency observations of Haller and Kramer [5] by computer analysis using the principle of minimization of total free energy, the sum of domain-wall energy which includes a frequency dependent term to account for domain wall bowing due to Lee's expression for the

wall profile with relevant assumptions of infinitesimal wall displacement and zero wall energy ingnored, and magnetoelastic energy of the static case. The main limitations of their theory are following;

(1) only valid for small wall displacements due to the assumption of constant permeability, and then the discrepancy between the cases of so-called "voltage excitation" and "current excitation" cannot be explained,

(2) domain spacing after ac demagnetization, $2a_0$, cannot be decided from the energy minimization approach, since the value of magnetoelastic constant is assumed as a function of $2a_0$.

In the present paper, the characteristics of the dynanic domain size variation regarding magnetizing frequency, demagnetizing frequency, peak flux density, and tape thickness in the cases of "voltage excitation" and "current excitation" in grain-oriented 3% Si-Fe tape wound cores are quantitatively analysed using the principle of minimization of total energy, the sum of domain-wall energy which is same in mathematical form as the result of Sharp and Horner [8] excepting the nonlinear permeability and magnetostatic energy at the boundaries of misaligned grains. And then the eddy-current losses under "voltage excitation" and "current excitation" versus magnetizing frequency, peak flux density, and demagnetizing frequency are calculated by using the results of the theoretical variation of dynamic domain size. These calculated values due to a digital computer are compared with the experimental results. The optimal tape thickness, at which the value of iron loss is minimum, is also derived using the calculated results of eddy-currnt loss and a model for hysteresis loss due to wall pinning.

2. FREE ENERGY COMPONENTS

The optimal domain size in a grain-oriented tape is that which leads to a minimum value for the sum of the free energies associated with the grain structures and the domain walls. Goodenough [9] (1954) has concluded that the surface density of magnetic poles at the grain boundaries ω^* is the most common source of domain nucleation energy in polycrystalline material, especially in that with large crystalline anisotropy such as Si-Fe tapes. It is difficult to calculate the magnetostatic energy of the dynamic domain pattern because the walls are not plane but are continually varying in profile. To simplify the analysis this energy component is approximated as for the static case. The magnetostatic energy per unit surface, E_{ms}, of a infinite crystal surface which is divided with equal width 180° domains has been expressed [10] as,

$$E_{mso}=1.704 M_s^2 \ 2a \qquad (\text{ergs}/\text{cm}^2)$$

where M_s and 2a are saturation magnetization and domain spacing.

This may be rewritten for unit volume of tapes, in which the number of grain boundaries is 1 / L(L : mean grain length in the rolling direction), to take account

of surface pole density at planar grain boundaries as,

$$E_{ms}=1.704\ \delta\ 2aM_s^2\ (1-\cos\phi)^2/L \qquad (1)$$

where ϕ is the average angle of the magnetization vectors in the domains apart from the rolling direction and δ is assumed as a parameter relating to the effect of spike domains, as shown in Fig. 1, which will reduce the value of surface pole density and the effect of finiteness of the area of a grain boundary which reduces the value of the demagnetizing factor in the rolling direction.

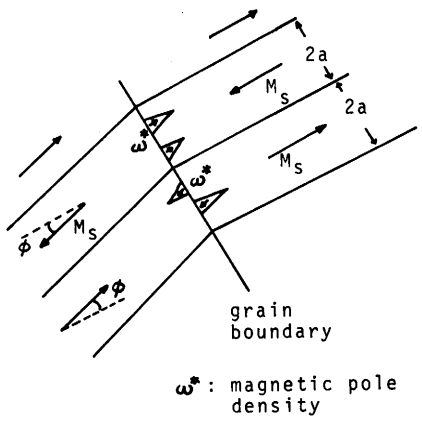

Fig. 1

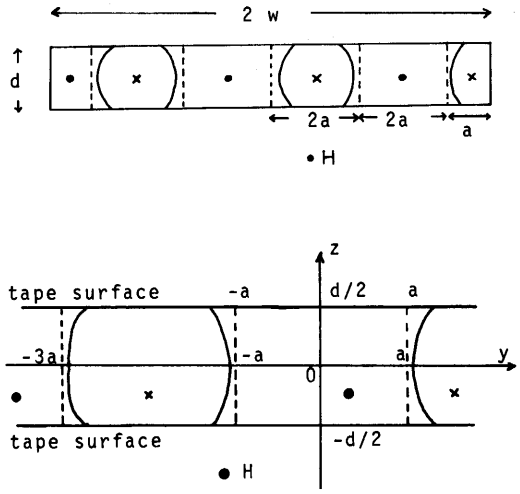

dynamic domain wall profile

Fig. 2

The average 180° domain-wall energy per unit volume over a cycle, E_w, is derived relating to a domain model as shown in Fig. 2 in the same manner as the result of Sharp and Horner [8] which is relating to Polivanov's domain model;

$$E_w=\varepsilon_m L_{mean}/2ad \qquad (2)$$

where ε_m and L_{mean} are mean energy per unit area of a bowing wall over a cycle and mean length of a bowing wall over a cycle respectively.

$$L_{mean}=\frac{1}{\pi}\int_{-d/2}^{d/2}dz\int_0^{\pi}\left[1+y_m^2\left(\frac{dp(z)}{dz}\cos\theta+\frac{dQ(z)}{dz}\sin\theta\right)^2\right]^{1/2}d\theta$$

$$\theta=\omega t$$

$$y_m=(adB_m/B_s)/F$$

$$F=\int_{-d/2}^{d/2}\left(P^2(z)+Q^2(z)\right)^{1/2}dz \qquad (3)$$

$$P(z)=1-64\xi^2\gamma^2\sum_{n=1}^{\infty}{}'A(z,n)/n$$

$$Q(z)=16\xi\gamma\sum_{n=1}^{\infty}{}'A(z,n)\tanh(n\pi\gamma)$$

$$A(z,n)=\pm\cos(n\pi z/d)/\pi(n^2\tanh^2(n\pi\gamma)+16\xi^2\gamma^2)$$

where $\gamma=a/d$, $\xi=\omega\mu_\Delta d^2/\rho$, and B_m/B_s is the normalized peak flux density.

The quasi-static permeability, μ_Δ, has been assumed constant in [8], but the value of μ_Δ is, in practice, a function of peak flux density. We represent, in this paper, the quasi-static permeability as a function of peak flux density by using a method of a describing function, which is frequently well known as an effective approach in dealing with nonlinear systems with ac excitation, for an approximated BH initial magnetization curves as shown in Fig. 3 as illustrated in Fig. 4 (see Appendix 1). The solid line is the quasi-static permeability in the case of $B=B_m\sin\omega t$ (voltage excitation), and the broken line is that in the case of $H=H_m\sin\omega t$ (current excitation)

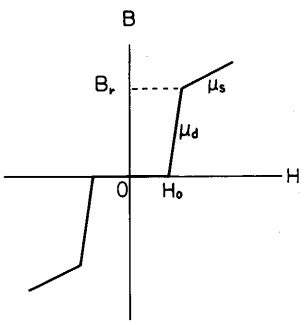

Fig. 3

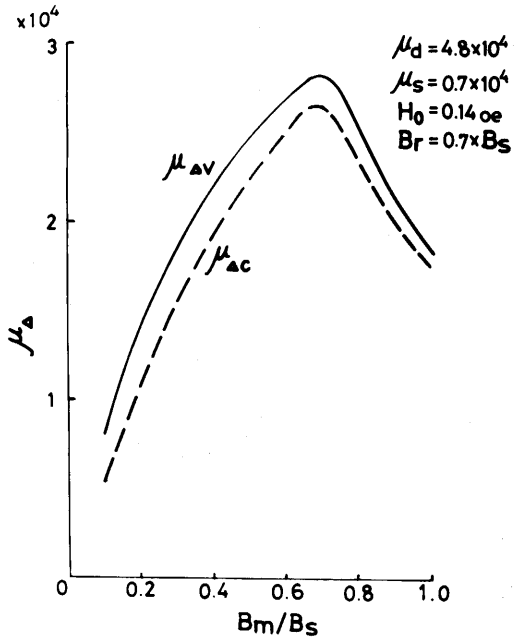

Fig. 4

3. ENERGY MINIMIZATION

The total spacing-dependent energy of the domain structure of Fig. 1 and Fig. 2 can be written as

$$E_t=E_{ms}+E_w \qquad (4)$$

The total energy E_t cannot be easily minimized by analytic means, since the mean wall length L_{mean} is a complex function of the domain-wall spacing. A numerical method was therefore adopted. The calculation of the summations involved the evaluation of the first 100 terms, and the calculation of the three times integrations in equation (3) are due to Gauss' method (see Appendix 2) .

4. DYNAMIC-DOMAIN SPACING

The theoretical curves from the numerical calculations are illustrated in Fig. 5, Fig. 6, and Fig. 7. The numerical values used in the calculations are shown in Table

Table 1.

B_s	1.7×10^4	gausses
d	0.01	cm
ρ	4.5×10^4	emu
ε_m	2.0	ergs/cm^2
ϕ	3°	
L	1.2	cm
δ	1	

1. The initial states at f=0 and $B_m/B_s=0$ in Fig 5 and Fig. 6 respectively are given as that the tape with 10mm width and 0.1mm thickness is reset in saturation and then is demagnetized with dc field. Since only one or two walls may exist in the tape after dc demagnetization in the same manner as observed in a long 3% Si-Fe single crystal [6] , the value of 2a/d is 50 at the initial state.

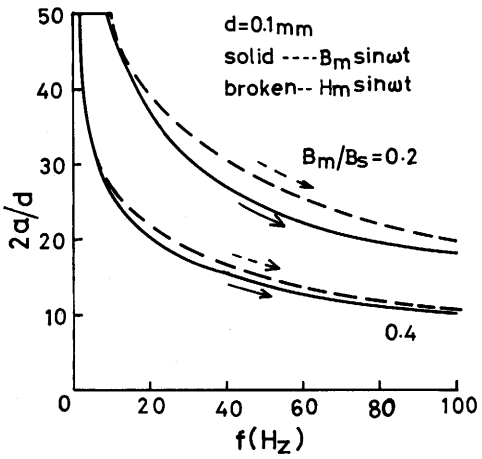

Fig. 5

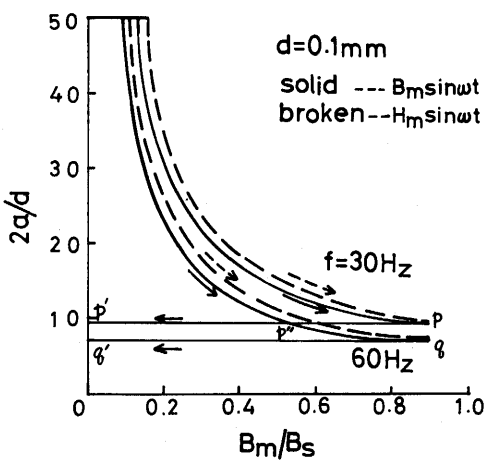

Fig. 6

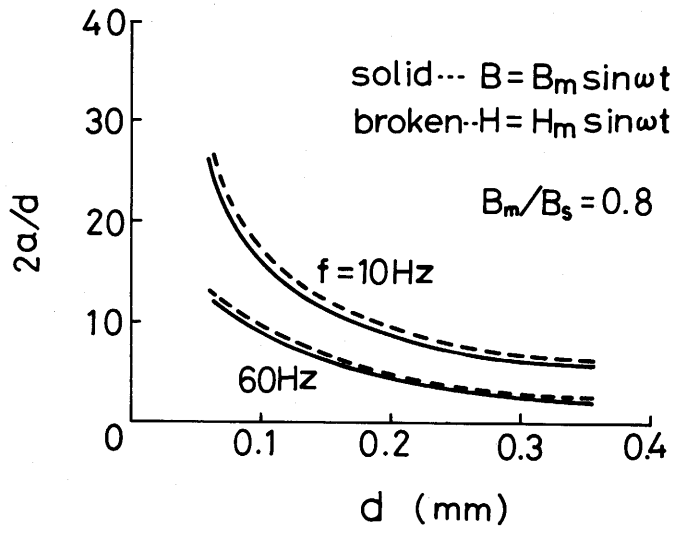

Fig. 7

It is found that the ratio of the domain spacing to the tape thickness decreases with the magnetizing frequency, the peak flux density, and the tape thickness for the both of "voltage excitation(solid lines)" and "current excitation(broken lines)". The values of 2a/d for "voltage excitation" are smaller than that for "current excitation". In ac demagnetizing process, 2a/d may vary from the point p to the point p′ for 30 Hz and from the point q to the point q′ for 60 Hz as shown in Fig. 6 since the total number of walls, nucleated with nearly saturated peak flux density, may be maintained as far as no domain-wall conjunction occurs. Then 2a/d varies along the curve p′→p″→q for the tape which is previously ac demagnetized with 30 Hz and then magnetized with 60 Hz.

Then the characteristics of 2a/d versus f, B_m/B_s, and are expressed in the following mathematical forms by logarithmic-logarithmic plotting the results of Fig. 5, Fig. 6, and Fig. 7;

$$2a/d=0.54\ (f)^{-0.45}\cdot(B_m/B_s)^{-0.90}\ d^{-0.9} \quad \text{for } B=B_m \sin\omega t \qquad (5)$$

$$2a/d=0.48\ (f)^{-0.40}\ (B_m/B_s)^{-0.95}\ d^{-0.9} \quad \text{for } H=H_m \sin\omega t \qquad (6)$$

we put $B_m/B_s=0.9$ in equations (5) and (6) for ac demagnetized states.

5. IRON LOSSES FOR VARIOUS DEMAGNETIZING FREQUENCIES AND MAGNETIZING CONDITIONS

We now express the iron losses of a 3% Si-Fe tape-wound core as the sum of the measured hysteresis losses and the calculated eddy-current losses. The hysteresis loss is obtained by integrating the area of a measured quasi-static BH loop using a planimeter. Fig. 8 and Fig. 9 show the experimental results of the hysteresis loss

versus demagnetizing frequencies, f_{dem}. It is found that the hysteresis loss is minimum at f_{dem}=600 Hz. The variation of the hysteresis loss with f_{dem} is considered due to the variation of the number of spike domains at grain boundaries because the incremental permeability of quasi-static BH loop is nearly independent of f_{dem}.

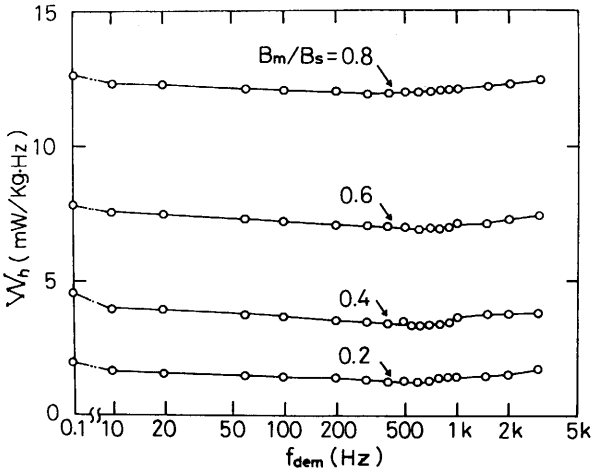

Fig. 8

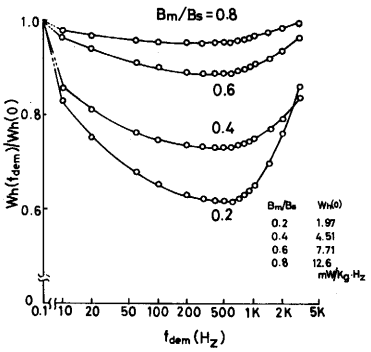

Fig. 9

The eddy-current loss per cycle in the tape of Fig. 2 is expressed in the following equation [3] ,

$$\frac{W_e}{f}=\frac{4\rho\xi^2\gamma B_m^2}{\mu_\Delta^2\pi^3F^2f}\sum_{n=1}^{\infty}{}'\frac{1}{n^3\tanh(n\pi\gamma)+16n\xi^2\gamma^2} \tag{7}$$

and is numerically calculated by substituting the values of μ_Δ and γ from Fig. 4 and equations (5) and (6) respectively into equation (7).

Fig. 10 shows the influence of demagnetizing frequency on the iron loss per cycle versus magnetizing frequency in a 3% Si-Fe tape-wound core (70 mm-outer diameter, 55 mm-inner diameter, 10 mm-tape width, and 0.1 mm-tape thickness) with "current excitation". The solid lines and the broken lines are theoretical values for previously dc demagnetized and ac demagnetized (f_{dem}=f) states, respectively. The chained lines are theoretical values for previously demagnetized state with f_{dem}=600 Hz, at which the hysteresis loss is minimum. The experimental values, measured the area of dynamic BH loops using a planimeter, for each demagnetized state are almost in agreement with the theoretical values. These lines are expressed in the following mathematical forms,

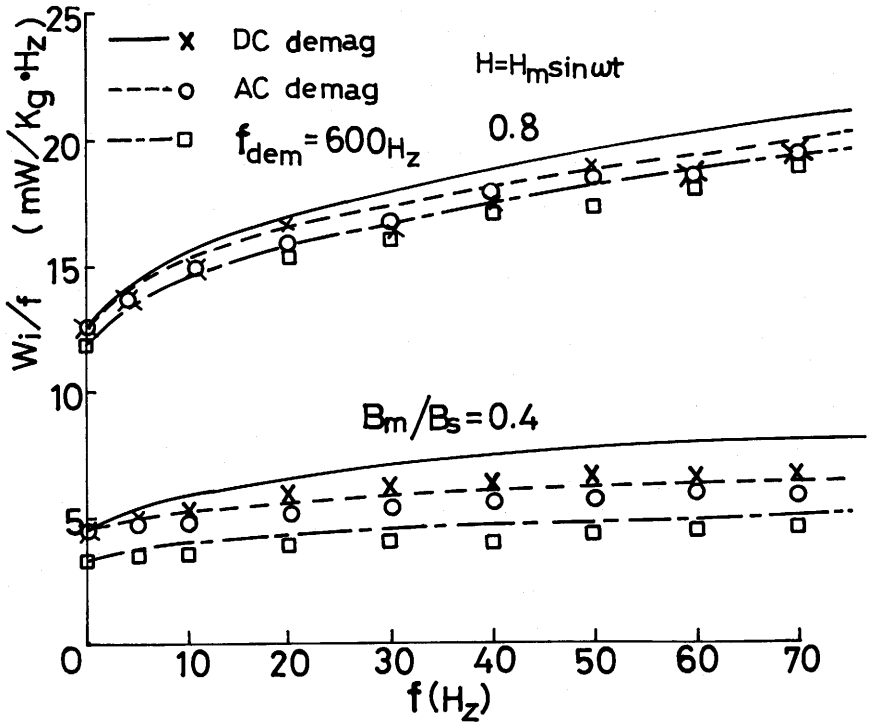

Fig. 10

$$W_e / f = 0.22\, f^{0.5}\, (B_m / B_s)^2 d^{1.1} \quad \text{for } f_{dem}=f \text{ and } f_{dem}=600 \text{ Hz} \tag{8}$$

$$W_e / f = 0.21\, f^{0.5}\, (B_m / B_s)^{1.2} d^{1.1} \quad \text{for dc demagnetized state} \tag{9}$$

Fig. 11 shows the influence of magnetiziing conditions on the iron loss per cycle versus magnetizing frequency in the core with $f_{dem}=f$. The soilid lines and broken lines are theoretical values for "voltage excitation" and "current excitation" respectively. The order of the magnitude of the both lines is in agreement with the experimental results.

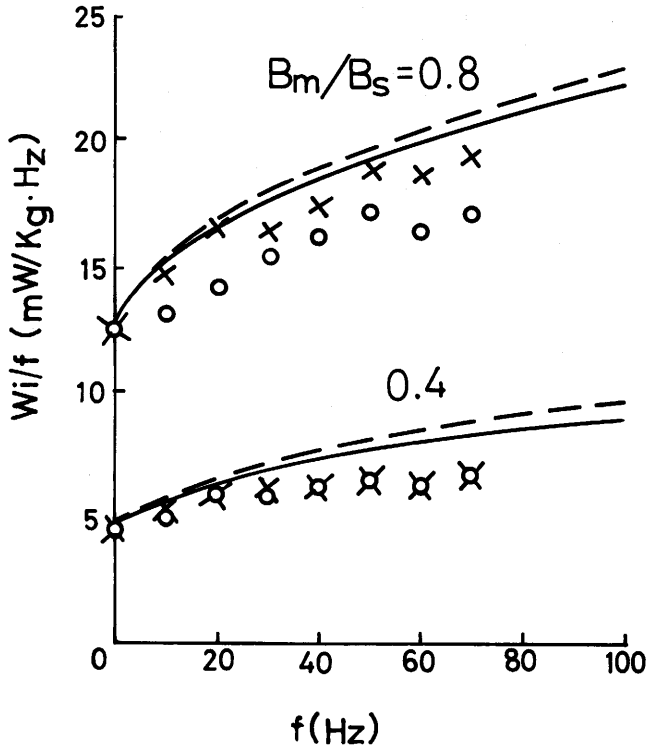

Fig. 11

6. OPTIMAL TAPE THICKNESS

Sharp and Overshott [11] (1973) have experimentally clarified the existence of optimum sample thickness of between 0.19 mm and 0.25 mm at 40 Hz, below which the iron losses rise rapidly.

We now assume the hysteresis for BH major loop as follows by approximating the shape of the loop as rectangular,

$$W_h = 4 B_s H_c \tag{8}$$

The coercive force has been expressed by Rodbell and Bean [12] (1956) using a wall-pinning model as

$$H_c = H_c^{int} + \varepsilon / M_s d \tag{9}$$

where H_c^{int} and ε are internal coercive force and wall energy density respectively. The hysteresis loss is therefore inversely proportional to the tape thickness. Then the total loss versus tape thickness in a 3% Si-Fe tape-wound core is calculated as shown in Fig. 12. It is found that the optimum tape thickness, at which iron loss is minimum, decreases with increasing magnetizing frequenncy and exists between 0.1 mm and 0.2 mm at power frequencies.

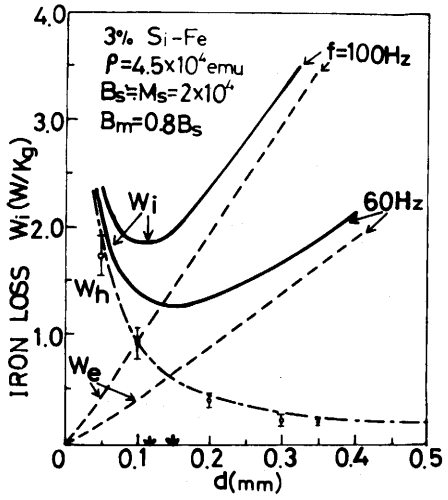

Fig. 12

7. CONCLUSIONS

1. The nonlinearity of the characteristics of the iron loss per cycle versus frequency (anomalous loss) is analysed by using a model for dynamic domain-spacing variation.

2. The ratio of the dynamic domain spacing to the tape thickness, the value of which is smaller at "voltage excitation" than at "current excitation", decreases with magnetizing frequency, peak flux density, and tape thickness.

3. The hysteresis loss is minimum at 600 Hz demagnetizing frequency in experiment.

4. The theoretical values for the influence of various demagnetizing frequency on iron-loss-per-cycle versus magnetizing frequency are in agreement with the experimental results.

5. The influence of magnetizing conditions on iron-loss-per-cycle versus magnetizing frequency is also calculated by using a model for domain-wall dynamics with a permeability as a function of peak flux density.

6. The optimum tape thickness between 0.1 mm and 0.2 mm for power frequencies, at which the iron loss is minimum, is calculated by using a model for wall pinning.

8. ACKNOWLEDGMENT

The author wishes to express his gratitude to Professor K. Harada of Kyushu University for his interest in this work and to Mr. T. Fujimoto, the technician of the Kyushu Institute of Technology, in the experimental work and to Mr. Y. Satoh, the graduate student, in the computation work.

REFERENCES

[1] H. Williams, W. Shockley and C. Kittel, "Studies of the Propagation Velocity of a Ferromagnetic Domain Boundary," Phys. Rev., Vol. 80, pp. 1090-1094, December 1950.

[2] R. H. Pry and C. P. Bean, "Calculation of the Energy Loss in Magnetic Sheet Materials Using a Domain Model," J. Appl. Phys., Vol. 29, pp. 532-533, March 1958.

[3] E. W. Lee,"Eddy-Current Effects in Rectangular Ferromagnetic Rods," Proc. IEE, Vol. 107c, pp. 257-264, April 1960.

[4] G. L. Houze, Jr., "Domain-Wall Motion in Grain-Oriented Silicon Steel in Cyclic Magnetic Fields," J. Appl. Phys., Vol. 38, pp. 1089-1096, March 1967.

[5] T. R. Haller and J. J. Kramer, "Observation of Dynamic Domain Size Variation in a Silicon-Iron Alloy," J. Appl. Phys., Vol. 41, pp. 1034-1035, March 1970.

[6] J. W. Shilling, "Domain Stucture in 3% Si-Fe Single Crystals with Orientation near(110) [001] ," IEEE Trans. on Magnetics, Vol. MAG-9, No. 3, pp351-356, Sept. 1973.

[7] T. R. Haller and J. J. Kramer, "Model for Reverse Domain Nucleation in Ferromagnetic Conductors," J. Appl. Phys., Vol. 41, pp. 1036-1037, March 1970.

[8] M. R. G. Sharp and J. T. Horner, "A Theoretical Analysis of the Frequency Dependence of Domain-Wall Spacing in a Ferromagnetic Sheet," J. Phys. D., Appi. Phys., Vol. 6, pp. 1835-1841, May 1973.

[9] J. B. Goodenough, "A Theory of Domain Creation and Coercive Force in Polycrystalline Ferromagnetics," Phys. Rev. Vol. 95, No. 4, pp. 917-932, August 1954.

[10] S, Chikazumi, "Physics of Ferromagnetism," (Book), P 150, 1965 (4th edition) Syokabo, Tokyo, Japan

[11] M. R. G. Sharp and K. J. Overshott, "Dependence of Power Loss on Lamination Thickness in 3% Grain-Oriented Silicon-Iron," Proc. IEE, Vol. 120, No. 11, pp. 1451-1453, November 1973.

[12] D. S. Rodbell and C. P. Bean, "Some Properties of the Coercive Force in Soft Magnetic Materials," Phys. Rev., Vol. 103, No. 4, pp. 886-895, August 1956.

APPENDIX 1

permeability as a function of B_m/B_s due to the describing function :

(a) $H=H_m \sin\omega t$

$$\mu_{dc}=\frac{\mu_d}{\pi H_m}\left[4H_o(\cos\phi_r-\cos\phi_0)+H_m(2\phi_o-\sin2\phi_r+\sin2\phi_o)+\frac{4}{\mu_d}(B_r-\mu_s H_r)\cos\phi_r+\frac{\mu_s}{\mu_d}H_m(\pi-2\phi_r+\sin2\phi_r)\right]$$

where, $\phi_0=\sin^{-1}(H_o/H_m)$ $\phi_r=\sin^{-1}(H_r/H_m)$

$H_r=H_o+B_r/\mu_d$

(b) $B=B_m\sin\omega t$

$$\mu_{dv}=\pi B_m/\left[4H_0(1-\cos\psi)+2(2H_r-B_r/\mu_s)\cos\psi+\frac{B_m}{\mu_d}(2\psi-\sin2\psi)+\frac{B_m}{\mu_s}(\pi-2\psi)\right]$$

where $\psi=\sin^{-1}(B_r/B_m)$

APPENDIX 2

```
FACOM 230-75 (M7)  FORTRAN-D    -74i130- V06-L03    75.10.25    PAGE  1

* SOURCE STATEMENT *

      C     DYNAMIC DOMAIN SIZE ( ET=EMS=EA IS MIN.) IN SILICON IRON TAPE CORE
      COMMON G,W,BM,H,Z,ZSIN,ZZCOS,P,T,A(36),X(36)
      T=3.141592
      AA=0.0
      R=1.571
      A(1)=1.0
      A(2)=0.3476548S
      A(3)=0.65214515
      A(4)=0.17132449
      A(5)=0.9607157
      A(6)=0.46791393
      A(7)=0.10122854
      A(8)=0.22238103
      A(9)=0.31370665
      A(10)=0.3622e837
      A(11)=0.66671344E-1
      A(12)=0.1494S135
      A(13)=0.21908936
      A(14)=0.26976672
      A(15)=0.2955922
      A(16)=0.47175336E-1
      A(17)=0.10693933
      A(18)=0.16067833
      A(19)=0.20316743
      A(20)=0.23349254
      A(21)=0.24914705
      A(22)=0.3511946E-1
      A(23)=0.80158087E-1
      A(24)=0.12151857
      A(25)=0.15720317
      A(26)=0.1e353840
      A(27)=0.20519846
      A(28)=0.21526385
      A(29)=0.2715745E-1
      A(30)=0.62253524E-1
      A(31)=0.95158512E-1
      A(32)=0.12462897
      A(33)=0.14959949
      A(34)=0.16915652
      A(35)=0.18260342
      A(36)=0.18945061
      X(1)=0.5773S027
      X(2)=0.8611361
      X(3)=0.3399810
      X(4)=0.9324695
      X(5)=0.661e0939
      X(6)=0.23661919
      X(7)=0.96028986
      X(8)=0.79866648
      X(9)=0.52553241
      X(10)=0.18343464
      X(11)=0.97390653
      X(12)=0.86506337
      X(13)=0.67940957
      X(14)=0.43339539
      X(15)=0.14887433
      X(16)=0.96156063
      X(17)=0.90411726
      X(18)=0.76590267
      X(19)=0.5b731795
      X(20)=0.3b783150
      X(21)=0.125233A1
      X(22)=0.98e283A1
      X(23)=0.92d43A88
      X(24)=0.82720132
      X(25)=0.6872929C
      X(26)=0.51524864
      X(27)=0.31911237
      X(28)=0.10805495
      X(29)=0.9b940093
      X(30)=0.94457502
      X(31)=0.86563120
      X(32)=0.75540441
      X(33)=0.61787624
      X(34)=0.45b01678
      X(35)=0.2d180355
      X(36)=0.95012510E-1

      SUBROUTINE GAUSC(C,D,N,V)
      COMMON G,W,BM,H,Z,ZSIN,ZZCOS,P,T,A(36),X(36)
      DIMENSION A1(16),X1(16)
      K=N
      IF(N-8) 10,30,20
   10 IF(N-1) 20,30,30
   20 K=8
   30 C1=(D+C)*0.5
      C2=(D-C)*0.5
      K2=K+K
      NK=K*(K-1)/2
      DO 40 J=1,K
      KJ=NK+J
      I=K2-J+1
      Y=C2*X(KJ)
      X1(J)=C1-Y
      X1(I)=C1+Y
      A1(J)=A(KJ)
   40 A1(I)=A(KJ)
      S=0.0
      DO 50 I=1,K2
      CALL FUNC(X1(I),ANS)
   50 S=S+A1(I)*ANS
      V=C2*S
      RETURN
      END

      SUBROUTINE FUNC(Z,ANS)
      COMMON G,W,BM,H,Z,ZSIN,ZZCOS,P,T,A(36),X(36)
      ZZSIN=SIN(Z)
      ZZCOS=COS(Z)
      AA=0.0
      R=H/2.0
      N=4
      CALL GAUSB(AA,R,N,VV)
      ANS=(2.0/1.571)*VV
      RETURN
      END

      N=4
      DO 21 J1=5,10,5
      DD=FLOAT(J1)/10.0
      WRITE(6,500) DD
  500 FORMAT(1H ,3HDD=,F7.2)
      DO 20 J=60,60
      NN=1
      JJ=101-J
      W=FLOAT(JJ)
      WRITE(6,200) W
  200 FORMAT(1H ,F7.2)
      DO 40 M1=11,51,5
      M=52-M1
      H=FLOAT(M)/1000.0
      WRITE(6,400) H
  400 FORMAT(1H ,F7.4)
      DO 31 L1=4,16,4
      L=20-L1
      V1=100.0
      BM=FLOAT(L)/20.0
      WRITE(6,300) BM
  300 FORMAT(1H ,F5.2)
      IF(L-18) 12,1,12
    1 P=2.11E4
   12 IF(L-16) 13,2,13
    2 P=2.48E4
   13 IF(L-14) 14,3,14
    3 P=2.79E4
   14 IF(L-12) 15,4,15
    4 P=2.61E4
   15 IF(L-10) 16,6,16
    6 P=2.39E4
   16 IF(L-8) 17,7,17
    7 P=2.13E4
   17 IF(L-6) 18,8,18
    8 P=1.79E4
   18 IF(L-4) 19,9,19
    9 P=1.3EA
   19 IF(L-2) 25,11,25
   11 P=0.79EA
   25 WRITE(6,600) P

  600 FORMAT(1H ,F12.5)
      DO 10 I=N,N+26
      G=FLOAT(I)
      CALL GAUSC(AA,B,N,V)
      GP=G*H
      EMS=2.24*2.0*GP*DD
      E=W*3.0*V
      ET=EMS*EW
      WRITE(6,100) I,GP,ET
  100 FORMAT(1H ,I3,5X,E13.6,5X,E13.6)
      IF(V1-ET) 30,5,5
    5 V1=ET
   10 CONTINUE
   30 CONTINUE
      NN=I-2
   31 CONTINUE
   40 CONTINUE
   20 CONTINUE
   21 CONTINUE
      STOP
      END

      SUBROUTINE GAUSB(C,D,N,V)
      COMMON G,W,BM,H,Z,ZSIN,ZZCOS,P,T,A(36),X(36)
      DIMENSION A1(16),X1(16)
      K=N
      IF(N-8) 10,30,20
   10 IF(N-1) 20,30,30
   20 K=8
   30 C1=(D+C)*0.5
      C2=(D-C)*0.5
      K2=K+K
      NK=K*(K-1)/2
      DO 40 J=1,K
      KJ=NK+J
      I=K2-J+1
      Y=C2*X(KJ)
      X1(J)=C1-Y
      X1(I)=C1+Y
      A1(J)=A(KJ)
   40 A1(I)=A(KJ)
      S=0.0
      DO 50 I=1,K2
      CALL FUNL(X1(I),ANS)
   50 S=S+A1(I)*ANS
      V=C2*S
      RETURN
      END

      SUBROUTINE FUNL(Z,ANS)
      COMMON G,W,BM,H,Z,ZSIN,ZZCOS,P,T,A(36),X(36)
      G2=G*G
      W2=W*W
      H2=BM*BM
      T2=T*T
      H2=H*H
      DD=(4.0*2.0*T**P*H2/4.5E4)*(4.0*2.0*T**P*H2/4.5E4)*G2
      AA=0.0
      R=H/2.0
      N=4
      S3=0.0
      S4=0.0
      DO 20 I=1,49,4
      FI=FLOAT(I)
      FF=FI*FI
      SS=SIN(FI*T*Z/H)/(T*(FF+DD))
      S3=S3+SS
      S4=S4+FI*SS
   20 CONTINUE
      S5=0.0
      S6=0.0
      DO 30 J=3,51,4
      F2=FLOAT(J)
      FF2=F2*F2
      SS2=SIN(F2*T*Z/H)/(T*(FF2+DD))
      S5=S5+SS2
      S6=S6+F2*SS2
   30 CONTINUE
      XX=2.0*T**P*H2/4.5E4
      XX2=XX*XX
      R=64.0*XX2*G2*(S3+S5)
      S=16.0*XX*W*(S4+S6)
      CALL GAUSA(AA,R,N,U)
      Y2=W+W+4.0
      RSZ=R*ZZCOS-S*ZZSIN
      RSZ2=RSZ*RSZ
      ANS=S*RT(1.0/(G2*H2)+T2*B2*RSZ2/Y2)
      RETURN
      END

      SUBROUTINE GAUSA(C,D,N,V)
      COMMON G,W,BM,H,Z,ZSIN,ZZCOS,P,T,A(36),X(36)
      DIMENSION A1(16),X1(16)
      K=N
      IF(N-8) 10,30,20
   10 IF(N-1) 20,30,30
   20 K=8
   30 C1=(D+C)*0.5
      C2=(D-C)*0.5
      K2=K+K
      NK=K*(K-1)/2
      DO 40 J=1,K
      KJ=NK+J
      I=K2-J+1
      Y=C2*X(KJ)
      X1(J)=C1-Y
      X1(I)=C1+Y
      A1(J)=A(KJ)
   40 A1(I)=A(KJ)
      S=0.0
      DO 50 I=1,K2
      CALL FUNK(X1(I),ANS)
   50 S=S+A1(I)*ANS
      V=C2*S
      RETURN
      END

      SUBROUTINE FUNK(Z,ANS)
      COMMON G,W,BM,H,Z,ZSIN,ZZCOS,P,T,A(36),X(36)
      G2=G*G
      B2=BM*BM
      W2=W*W
      H2=H*H
      T2=T*T
      DD=(4.0*2.0*T**P*H2/4.5E4)*(4.0*2.0*T**P*H2/4.5E4)*G2
      S1=0.0
      S2=0.0
      DO 10 I=1,49,4
      FI=FLOAT(I)
      FF=FI*FI
      SC=COS(FI*T*Z/H)/(T*(FF+DD))
      S1=S1+SC/FI
      S2=S2+SC
   10 CONTINUE
      S3=0.0
      S4=0.0
      DO 20 J=3,51,4
      F2=FLOAT(J)
      FF2=F2*F2
      SM=-COS(F2*T*Z/H)/(T*(FF2+DD))
      S3=S3+SM/F2
      S4=S4+SM
   20 CONTINUE
      XX=2.0*T**P*H2/4.5E4
      XX2=XX*XX
      O=1.0-64.0*XX2*G2*(S1+S3)
      Q=16.0*XX*G*(S2+S4)
      ANS=SQRT(O**2+Q**2)
      RETURN
      END
```